Study on the Law of Durability and Fracture Energy of Structural Engineering Cement Mortar in Sulfate Erosion

Yijie Zhang [2], Miaojun Sun[1,3,a,*],Zixuan Zhang [2], HaoJiang[2],Xingzhi Ba[2,b,*]

[1]Powerchina Huadong Engineering Corporation Limited,310000,Hangzhou,China
[2]School of Qilu Transportation Engineering, Shandong University, 250101, Jinan, China
[3]Zhejiang Engineering Research Center of Marine Geotechnical Investigation Technology and Equipment,310000,Hangzhou,China

Corresponding author's e-mail address:[a]sun_mj2@hdec.com,[b]xingzhi_ba@sdu.edu.cn

Abstract. The durability of cement mortar in structural engineering is very important to the structural safety and stability, especially under the action of sulfate erosion, and the deterioration speed is faster and more serious. However, the fracture performance of mortar is not clear, so this paper studies the durability and fracture energy law of cement mortar in structural engineering in the process of sulfate erosion.The sulfate corrosion test of ordinary Portland cement mortar with water- cement ratio of 0.4, 0.5 and 0.6 was carried out. The appearance damage of specimens was observed at different erosion ages and the content of sulfate ions in the samples was measured. And the permeability and transmission law of sulfate in cement mortar were studied. The results show that the sulfate attack on the mortar is from the surface to inside, and the smaller the water cement ratio is, the stronger the ability to resist sulfate attack. With the deep penetration depth, the free sulfate ion content And the content of free sulfate ions decreased with the decrease of water-cement ratio. In contrast, the content of sulfate ions in the reaction increased first and then decreased, and finally stabilized. For the mortar surface, the smaller the water-cement ratio, the more the content of sulfate ions, and for the mortar interior, high water-cement ratio of the reaction of the sulfate ion content of the reaction is higher. In the fracture energy aspect, the test pieces with small water-cement ratio first increase and then decrease, and the bigger the water-cement ratio is, the shorter the age of fracture initiation is.

Keywords: sulfate ions; water-cement ratio; cement mortar; permeability; fracture energy

1 PREFACE

Sulfate corrosion is an important part of the durability of concrete, and it is also the most complex and harmful factor affecting it. Environmental water erosion: soil, groundwater, seawater, decayed organic matter and industrial wastewater all contain

B. Yuan et al. (eds.), *Proceedings of the 2024 8th International Conference on Civil Architecture and Structural Engineering (ICCASE 2024)*, Atlantis Highlights in Engineering 33,
https://doi.org/10.2991/978-94-6463-449-5_41

sulfate ions. They penetrate into the concrete and react with the cement hydration products, causing the concrete to expand, crack, peel, etc., thus causing the concrete to deteriorate. Loss of strength and tack. In recent years, the problem of sulfate corrosion has been discovered in highways, seaports, airports and other projects. In severe cases, it can even cause structural damage to concrete structures, causing buildings to fail prematurely before reaching their expected design service life. Causing huge losses of human and financial resources. Therefore, the problem of concrete sulfate corrosion has attracted more and more attention from scientific researchers and engineering and technical personnel [1].

Since the 1850s, my country has begun to conduct research on sulfate corrosion. In recent years, domestic experts and scholars have achieved a large number of research results through continuous in-depth research on sulfate corrosion. Han Yudong, Zhang Jun, Gao Yuan[2] and others reviewed the research on concrete's resistance to sulfate corrosion and pointed out that in actual projects, the material composition of concrete itself and the sulfate corrosion environment are different. Starting from the factors of concrete salt invasion type and erosion speed, systematically analyzed the research status of concrete sulfate corrosion at home and abroad, and put forward corresponding engineering protection suggestions. Jin Zuquan, Zhao Tiejun[3] et al. immersed and dried cyclic corrosion damage on concrete in magnesium sulfate solution and Qinghai Salt Lake brine. The test results showed that the combined action of sulfate ions and magnesium ions in the corrosive solution caused concrete to spall; its relative dynamic elasticity As the erosion time increases, the modulus and weight first decrease, then maintain equilibrium, and finally decrease at an accelerated rate. Yang Quanbing, Yang Qianrong[4] and others studied the physical erosion of sodium sulfate on the crystallization in the capillary pores of concrete, and proposed that the crystallization pressure of sodium sulfate under cooling can exceed 7MPa, which greatly exceeds the tensile strength of concrete. However, they rarely study the penetration of free sulfate radicals and reacted sulfate radicals separately. The diffusion range of the total sulfate ion and the content of the reactive sulfate are very important for the analysis of the cracking mechanism of cement mortar. This article explains the transmission mechanism of sulfate radicals by measuring free sulfate radicals and reacted sulfate radicals.

2 TEST OVERVIEW

2.1 Raw Materials

Material selection is consistent with the materials used in the engineering.This test uses P.O42.5 ordinary Portland cement produced by a cement factory in Qingdao. The performance indicators of cement are shown in Table 1; the fine aggregate is Qingdao local river sand, the maximum particle size is 5mm, and the fineness modulus of medium sand is 2.6; the water-reducing agent is polycarboxylic acid high-efficiency water-reducing agent; the water is Qingdao City Drinking tap water; the test specimens adopt three water-cement ratios of 0.4, 0.5, and 0.6. The test specimen sizes include 40mm×40mm×160mm prism specimens and 70.7mm cubic specimens with a side length. The detailed coordination ratio is shown in Table 2.

Table 1. Chemical composition of ordinary Portland cement

Chemical composition of ordinary Portland cement (%)	SiO_2	Fe_2O_3	Al_2O_3	CaO	MgO	SO_3	K_2O	Na_2O	TiO_2	P_2O_5
P.O 42.5R	22.91	3.1	7.35	57.46	4.07	1.52	0.47	0.99	0.35	0.05

Table 2. Mortar mix ratio

Mortar type	Cement type	Water-cement ratio(kg/m^3)	Cement(kg/ m^3)	Water consumption (kg/ m^3)	Sand (kg /m^3)	Water reducing agent
A	P.O	0.4	450	180	1350	1.3%
B		0.5	450	225	1350	0.90%
C		0.6	450	270	1350	—

2.2 Test Methods

After the mortar specimens underwent standard curing for 28 days, the sulfate corrosion test was started. The sulfate test was carried out in accordance with the "Test Method for Cement Resistance to Sulfate Attack" (GB/T749-2008)[5]. A group of three mortar specimens with different water-cement ratios were immersed in a sodium sulfate solution with a mass fraction of 5% and tap water for 28d, 60d, 90d, and 180d respectively, with tap water serving as the control group. In order to ensure that the solution has a stable pH value, the solution is updated once a month[6]. When reaching the corresponding age, observe the appearance changes of the specimens with different water-cement ratios, and take out a group of specimens for each water-cement ratio for permeability testing[7].

2.2.1 Sulfate Penetration Depth Test.

(1) Test sample preparation

After the mortar specimen reaches the soaking age, take it out and place it at a temperature of 50±2°C for drying. Using a layered grinder, according to the layered grinding method, the eroded surface of the cube specimen with a side length of 70.7mm was ground in layers, with a grinding depth of 20mm. The layers are every 1mm for the front 10mm, and every 2mm for the back 10mm[8]. Collect the ground powder from each layer and pass it through a standard sieve (aperture: 0.63mm) and seal it in a #5 sealed bag for later use.

(2) Determination of sulfate ion concentration

The UV spectrophotometer used in this experiment is the UV-5500 photometer produced by Shanghai Precision Instrument Manufacturing Company. Its working principle is that the energy in the atoms and molecules in the material is excited by light and

other various effects. The interaction between these forms and light results in the absorption of light. Since different substances have different needs for light, they have their own absorption spectra[9].

The measurement of the spectrophotometer is based on the principle of relative measurement. The calibration solution is selected and the transmittanceτis assumed to be 100%. Therefore, the transmittance τ of the test sample is a measured value relative to the standard medium. Within a certain range, it follows Lambert's law (Equations 1~2):

$$T(\tau)=I/I_0 \quad (1)$$

$$A=KCL=lg\tau \quad (2)$$

where T(τ) is the transmittance

A: Absorbance

C: concentration of solution

K: Absorption coefficient of solution

L: The length of the liquid layer in the optical path

I: The intensity of light that passes through the test sample and irradiates onto the photoelectric converter

I_0: The intensity of light that passes through the standard sample and irradiates the photoelectric converter.

The spectrophotometer will refer to Lambert's law and contain a functional equation in its internal calculator. Therefore, you only need to enter the concentration value of the standard sample or the coefficients M and N in the functional relationship to directly measure the unknown concentration value [10].

(3) Test process

(1) Preparation of reagents: ① $BaCl_2$-PVA solution: Weigh 60.0g BaCl2 and 50g and add to distilled water, stir and heat until completely dissolved, and adjust the volume to 1000ml; ② Prepare 2.5mol/L HCl solution for later use.

(2) Experimental steps: ① Take 2g of powder packed in a #5 sealed bag, soak it in 50ml of distilled water or dilute nitric acid (concentrated nitric acid: water = 15:85), and place it on a oscillator to shake for 30 minutes and rest for 24 hours; ② Use medium-speed filter paper to filter the test, take 25ml of the filtrate and add it to the colorimetric tube; ③Add 2.5ml of dilute HCl to the colorimetric tube, then add 10ml of BaCl2-PVA solution, and then adjust the volume to 50ml with distilled water or dilute nitric acid, and shake it by hand for 2 , 3 times to distribute the precipitate evenly and let it stand for 5 minutes; add an appropriate amount of the ④area into the cuvette and measure the absorbance.

2.2.2 Fracture Energy Test Method.

(1) Test piece type

The three-point bending test is performed as shown in Figure 1. The size of the mortar specimen is 40 mm×40 mm×160 mm, and the two-point support distance Lz is 150 mm. After the specimen is dried, the initial crack is cut with a diamond saw, and the crack height ratio is (a /h) is 0.5.

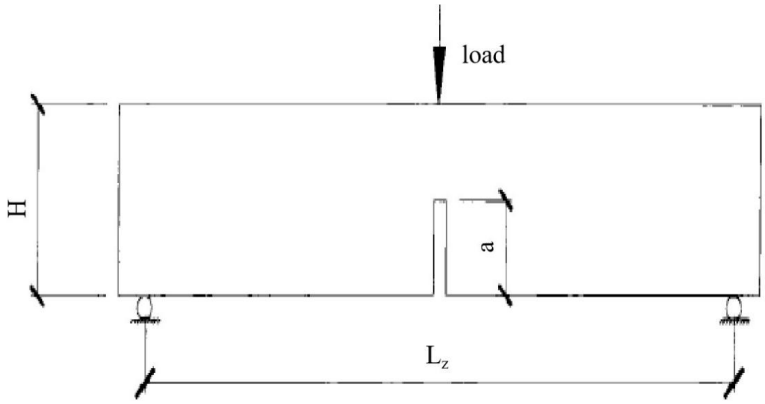

Fig. 1. Schematic diagram of loading of three-point bending test specimen

(2) Test process

The test was carried out on a computer-controlled Shimadzu 250KN universal testing machine. A rigid bracket was placed on the top surface of the specimen and matched with the iron parts on both sides bonded to the bottom of the specimen. It was used to fix the extensometer for measuring the bending deflection of the specimen and measure the span. Medium deflection. During the test, first measure the self-weight W of the specimen, accurate to 1N, and then place the specimen. The loading speed is 0.3mm/min. The test results are synchronously recorded by an online computer, and the load-deflection curve of the three-point bending test can be directly obtained[11].

(3) Evaluation of test results

The fracture energy of the three-point bending beam is calculated according to Equation (3);

$$G_F=(E+W\delta_0)/A_{lig} \quad (N/m) \tag{3}$$

In the formula: E——the area enclosed by load-deformation and coordinate axis;

W——Linear density of beam;

δ_0——Deflection deformation of the specimen when it finally fails;

A_{lig} ——area of ruptured ligament.

(4) Test data processing

When conducting the fracture energy test, in order to reduce the test error, the method of averaging the curves of three specimens is used. The raw data obtained can be used to obtain an average curve through the Origin software. After processing the original data, CONSOFT software was used to fit the average curve. This software uses the reverse analysis method as the basic principle. By continuously adjusting parameters, it has achieved the purpose of fitting, and finally obtained the strain softening curve and fracture energy.[12]

3 TEST RESULTS AND ANALYSIS

3.1 Appearance Damage of Mortar

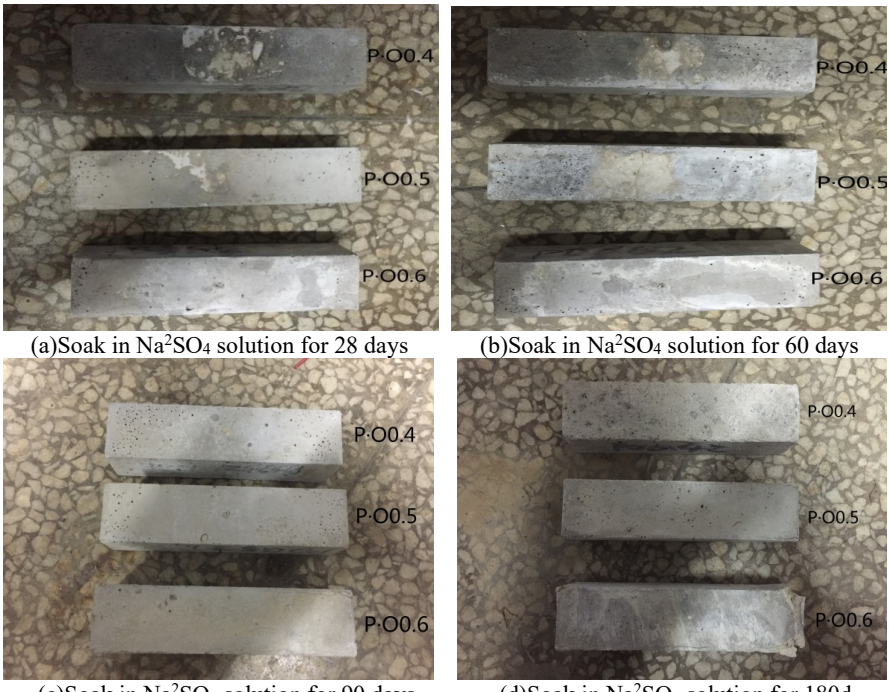

(a)Soak in Na^2SO_4 solution for 28 days (b)Soak in Na^2SO_4 solution for 60 days

(c)Soak in Na^2SO_4 solution for 90 days (d)Soak in Na^2SO_4 solution for 180d

Fig. 2. Surface changes of each group of specimens during immersion at different stages.

Figure 2 reflect the conditions of the mortar specimens soaked in sodium sulfate solution at each stage after soaking for 180 days. There was no obvious swelling and cracking phenomenon in the specimens soaked in sodium sulfate solution for 28 days and 60 days. After soaking for 90 days, 0.6 The water-cement ratio specimen showed longer cracks at the edges, and the cement mortar at the edges became brittle and easily peeled off. However, there were no obvious signs of corrosion at the water-cement ratios of 0.4 and 0.5. After being soaked for 180 days, it can be seen that the 0.6 water-cement ratio specimen has undergone obvious damage. The end of the specimen expanded and cracked in a radial shape, accompanied by severe peeling, and the cracking has extended to the entire edge. After 180 days of immersion, the 0.5 water-cement ratio specimen also developed cracking at the edges and corners, but it was much less severe than the 0.6 water-cement ratio specimen. However, the specimen with a water-cement ratio of 0.4 still showed no obvious signs of surface damage.

The above test phenomena show that the water-cement ratio plays a very critical role in the resistance to sulfate corrosion of mortar specimens. The smaller the water-cement ratio, the stronger the resistance to sulfate corrosion. The corrosion of mortar specimens by sulfate is from the surface to the inside. The erosion is first manifested at the edges

and corners. The cement stones at the edges and corners appear loose, crispy, cracked and peeled. As sulfate ions continue to invade, the entire mortar specimen will Complete fragmentation occurs.

3.2 Penetration and Transmission Rules of Sulfate in Mortar

3.2.1 Results and Analysis of Water-Cement Comparison and Free Sulfate Ion Content.

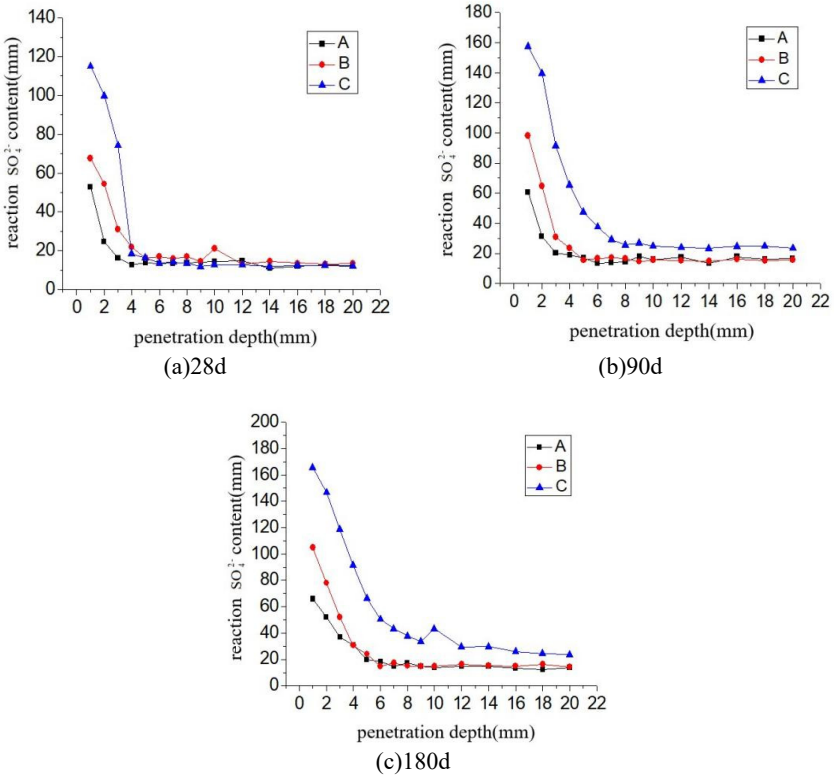

Fig. 3. Curve of free sulfate ion content with penetration depth at different soaking ages

The solution absorbance values measured by a UV spectrophotometer were substituted into formulas (1) and (2) respectively to obtain the free sulfate ion and total sulfate ion contents of the mortar powder in water-soluble and acid-soluble conditions.

Figure 3 reflects the change in free sulfate ion content with penetration depth when ordinary Portland cement mortar specimens with different water-cement ratios (0.4, 0.5 and 0.6) are soaked in 5% sulfate solution for different ages. It can be seen from the above figures that the content of sulfate ions on the surface of mortar specimens with different water-cement ratios is relatively high. As the penetration depth increases, the content of free sulfate ions first continuously decreases and then becomes stable, and

at the same penetration At depth, the smaller the water-cement ratio, the smaller the content of free sulfate ions, which reflects the better its impermeability. The reason is that as the water-cement ratio increases, the porosity of the mortar specimen decreases, and water penetration will inevitably be hindered to a certain extent. The sulfate ions entering the interior of the mortar specimen with water will also decrease accordingly. As the water-cement ratio decreases, the proportion of cement in the mortar specimen further increases, which results in an increase in substances such as C3A that can react with sulfate ions and consumes a large amount of free sulfate ions, so it exhibits The free sulfate content will be reduced accordingly. When soaked for 28 days, the penetration depth of sulfate ions inside the mortar is about 4~5mm; when soaked for 90 days, the penetration depth of sulfate ions inside the mortar is about 6~8mm; when soaked for 180 days, the penetration depth of sulfate ions inside the mortar is about 7~10mm. . It can be seen that as the sulfate corrosion age increases, the penetration depth of free sulfate ions inside the mortar also increases.

3.2.2 Results and Analysis of Sulfate Ion Content in Water-Cement Comparison Reaction.

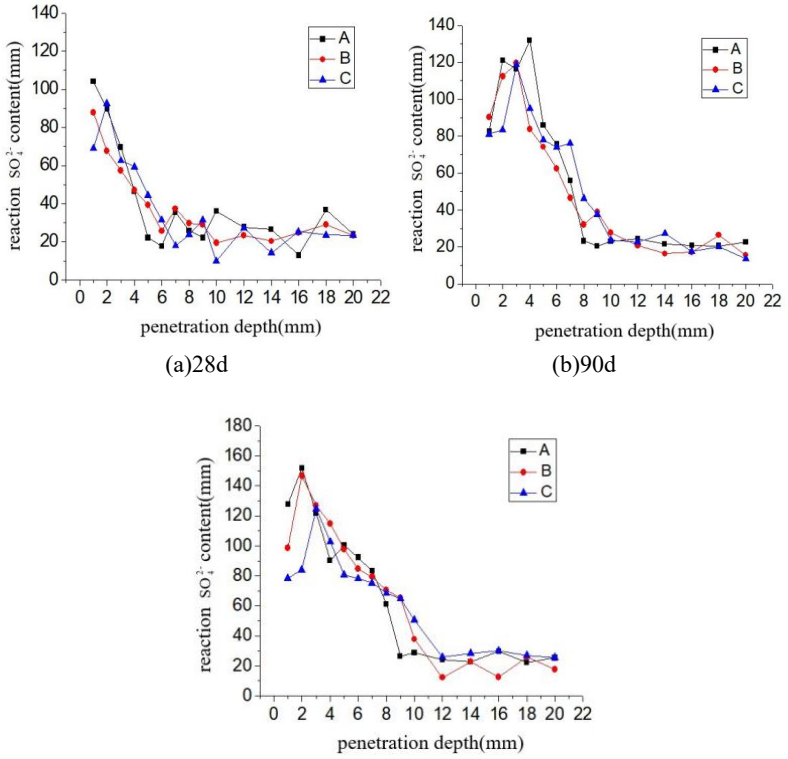

Fig. 4. Change curve of sulfate ion content with penetration depth in response to different soaking ages

Reactive sulfate ions reflect the content of corrosion products such as ettringite generated when sulfate ions enter the interior of the mortar and react with the hydration products of the cement. Figure 4 reflects the variation in the content of reacted sulfate ions with penetration depth when cement mortars with different water-cement ratios (0.4, 0.5 and 0.6) are soaked in 5% sulfate solution for different ages. It can be seen from the above figures that as the penetration depth deepens, the reactive sulfate ion content of mortar specimens with different water-cement ratios generally shows an overall trend of first increasing, then decreasing, and finally stabilizing. When the penetration depth of the first two or three layers of mortar is high, the content of reacted sulfate ions inside the mortar is higher, and the content of reacted sulfate ions in the surface layer is less than that in the second layer. This is because as the erosion age increases, a large amount of Ca (OH)2 is consumed, and the alkalinity of the concrete decreases, causing the ettringite to become unstable and decompose due to dehydration.[13-15] Part of the ettringite is converted from the AFt phase to the AFm phase, and at the same time, hydrated calcium silicate is generated and is dissolved with the erosion solution [16-19]. And in the first few layers of penetration depth, the lower water-cement ratio contains higher reactive sulfate ions, that is, the content of corrosion products such as ettringite inside the low water-cement ratio mortar is higher. And the smaller the water-cement ratio, the greater the content of reacted sulfate ions, that is, the more corrosion products such as ettringite are generated inside the mortar[20]. This is because in low water-cement ratio mortar, cement accounts for a larger proportion, and the C3A content in cement clinker is higher, resulting in more corrosion products such as ettringite generated by the reaction between its hydration products and sulfate ions, and the final performance Because of the high content of sulfate ions in the reaction[21]. As the penetration depth increases, the reactive sulfate ion content of the low water-cement ratio mortar specimen is gradually lower than that of the high water-cement ratio mortar. The reason is that as the penetration depth increases, due to the larger internal porosity of the high water-cement ratio mortar, the sulfate ions Ions are more likely to invade deep into the mortar, so high water ash reacts to produce more corrosion products than the mortar, which is manifested by a higher content of reacted sulfate ions[22].

3.3 Fracture Behavior Test Results and Analysis

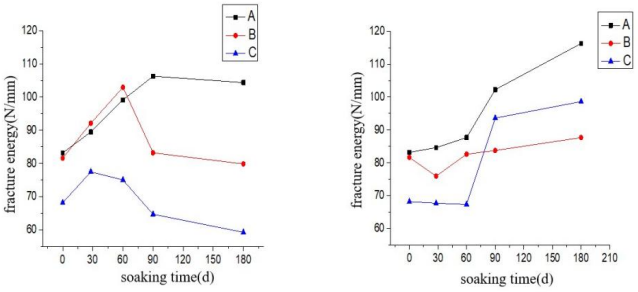

(a) Specimen immersed in Na_2SO^4 (b) Specimen immersed in water

Fig. 5. Curve of specimen fracture energy changing with time

It can be clearly seen from Figure 5 that the fracture energy of the specimen is a process of first increasing and then decreasing. Although the fracture energy of the mortar specimen soaked in water also shows an overall upward trend, it can be seen from the figure that the fracture energy of the specimen soaked in water shows an overall upward trend. For specimens in sodium sulfate solution, the fracture energy increases rapidly in the early stage. This trend is basically the same as the change trend of strength, and both are consistent with the characteristics of sulfate corrosion. However, it can be seen from Figure 5(a) that the fracture energy of the specimen with a water-cement ratio of 0.5 and 0.6 increases and decreases significantly, while the fracture energy of the specimen with a water-cement ratio of 0.4 reaches its maximum value after immersion for 90 days. There is a slight downward trend after 90 days. From this aspect, it can be explained that the higher the water-cement ratio, the lower the ability of the specimen to resist fracture energy. In addition, the compression and flexural resistance of the mortar specimen with a water-cement ratio of 0.4 has always been at the same level. Compared with the growth state, its fracture energy began to decline slightly, indicating that the fracture energy is forward-looking in predicting the hazards of sulfate erosion of cement-based materials such as mortar.

To explain the change in fracture energy from an energy perspective, with the continuous intrusion of sulfate ions, ettringite continues to form. In the initial stage, ettringite fills the gaps. During the stretching process, the internal ettringite will be squeezed. Absorbing part of the energy, this causes the mortar fracture energy to increase in the initial stage; as the ettringite continues to increase, its internal pressure does positive work during the entire stretching process, reducing the work done by the external tensile force. Assuming the area of the broken ligament Under the same circumstances, according to formula (4), it can be seen that when the external force work decreases, the concrete fracture energy decreases[23].

$$G_F=W_F/A_{lig} \tag{4}$$

In the formula: WF——external force work or fracture energy;

A_{lig}——ruptured ligament area.

To explain the change in fracture energy from the perspective of strength, the change in strength can be divided into two stages, namely the rising stage and the falling stage. First, let's look at the rising stage. With the intrusion of sulfate ions, ettringite is formed to fill the internal pores. During the stretching process, ettringite generates a certain friction force between the pores and the inner wall of the pores, thereby increasing the distance between the cementitious material and the inner pore wall. The biting force of fine aggregate forms an obvious crack bridge mechanism, which increases the fracture energy; when ettringite continues to form, its expansion force is significantly greater than the friction on the inner wall of the pores, and the crack bridge mechanism becomes extremely weakened, thus Reduce the fracture energy.

4 CONCLUSION

(1) Sulfate attacks mortar specimens from the outside to the inside. The smaller the water-cement ratio, the stronger the ability to resist sulfate erosion.

(2) The content of sulfate ions on the surface of mortar specimens with different water-cement ratios is relatively high. As the penetration depth increases, the content of free sulfate ions first decreases and then becomes stable. At the same penetration depth, the water-cement content The smaller the ratio, the less the content of free sulfate ions, which reflects the better its impermeability.

(3) As the penetration depth deepens, the reactive sulfate ion content of mortar specimens with different water-cement ratios generally shows an overall trend of first increasing, then decreasing, and finally stabilizing. In the first few layers of penetration depth, the smaller the water-cement ratio, the greater the content of reactive sulfate ions. As the penetration depth increases, the content of reactive sulfate ions inside the high water-cement ratio mortar gradually increases.

(4) After sulfate ions invade the mortar specimen, the change in fracture energy of the specimen first increases and then decreases, and the influence of sulfate ions on the fracture energy of the mortar specimen is greatly affected by the water-cement ratio.

(5) In this paper only for the natural erosion of sulfate cement mortar in the penetration and fracture of studied, mainly reveals the high concentration of sulfate ions in cement mortar diffusion and its inferior effect, but on the internal microstructure, subsequent will combine the microscopic change, the inferior effect of sulfate ions.

ACKNOWLEDGEMENTS

This article was funded by National key R&D plan(NO. 2022YFB2603300、NO.2022YFB2603303),Shandong Excellent Youth Fund(NO.ZR2022YQ56),Science and Technology Research and Development Plan Project of China National Railway Group Co., Ltd (NO. K2021G021),Shandong Natural Science Foundation General Project (No. ZR2023ME235)、The Taishan Scholars Program,Ministry of Housing and Urban-Rural Development(No.2020-K-142),Shandong Province Housing and Urban-Rural Construction Science and Technology Plan Project(No.2019-S7-1,No.2020-Z2-1),Shandong Provincial Key Research and Development Program(No. 2021CXGC010209),Shandong Provincial Department of Transportation science and technology project(No.2020B05).National Natural Science Foundation of China (No.52308407).

REFERENCES

1. Zhang Yijie, Zhao Tiejun. Research on the influence of sulfate erosion environment on the fracture properties of cement-based materials [D]. Qingdao University of Technology, 2013, 12.
2. Han Yudong, Zhang Jun, Gao Yuan. Review of research on concrete's resistance to sulfate corrosion[J]. Concrete, 2011. (1)
3. Jin Zuquan, Zhao Tiejun, et al. Research on sulfate corrosion of slag concrete [J]. Journal of Qingdao University of Science and Technology, 2009, 30(4):75-78, 86.
4. Yang Quanbing, Yang Qianrong. Effect of sodium sulfate crystallization on concrete damage[J]. Journal of Ceramics, 2007, 35(7).

5. Liu Hongzhu, Zhao Tiejun, et al. Experimental study on expansion rate of cement mortar under sulfate erosion environment [J]. 2015, (5): 41-43
6. Zheng Feng, Qin Guoshun. Research status of environmental factors of concrete sulfate corrosion[N]. Journal of Xuzhou Institute of Technology, 2010, 3(1).
7. Liu Chongxi et al. Evolution of crystal structure during dehydration of ettringite[J]. Proceedings of the Yangtze River Academy of Sciences, 1989, (3): 60-67.
8. Liu Hongzhu, Zhao Tiejun. Research on the effects of freeze-thaw and sulfate effects on cement mortar damage[D]. Qingdao University of Technology, 2013, 12.
9. Sadagopan M ,Rivera O A ,Malaga K , et al.Recycled Fine and Coarse Aggregates' Contributions to the Fracture Energy and Mechanical Properties of Concrete[J].Materials,2023,16(19):
10. Ludwik G G .Fracture Performance of Cementitious Composites Based on Quaternary Blended Cements[J].Materials,2022,15(17):6023-6023.
11. Giao V ,Fabian D ,J. J T , et al.Reduced Order Multiscale Simulation of Diffuse Damage in Concrete[J].Materials,2021,14(14):3830-3830.
12. Ahmed A M ,H. F A S ,H. K Y , et al.Mechanical and Fracture Parameters of Ultra-High Performance Fiber Reinforcement Concrete Cured via Steam and Water: Optimization of Binder Content[J].Materials,2021,14(8):2016-2016.
13. Raffaele C ,Angelo A ,Federico A , et al.Size-scale effects and modelling issues of fibre-reinforced concrete beams[J].Construction and Building Materials,2023,392.
14. Alireza M H ,Seyedmahdi A ,Reza M E .Fracture characteristics of various concrete composites containing polypropylene fibers through five fracture mechanics methods[J].Materials Testing,2023,65(1):10-32.
15. Alireza D ,Mohsen G ,Chengbin D .A fracture energy–based viscoelastic–viscoplastic–anisotropic damage model for rate-dependent cracking of concrete[J].International Journal of Fracture,2022,241(1):1-26.
16. Chen Y ,Zhang J ,Ma J , et al.Tensile strength and fracture toughness of steel fiber reinforced concrete measured from small notched beams[J].Case Studies in Construction Materials,2022,17.
17. Farzad H ,Hogr K ,Hamid K , et al.Fracture mechanics modeling of reinforced concrete joints strengthened by CFRP sheets[J].Case Studies in Construction Materials,2022,17.
18. Abedulgader B ,Henrik B .Fracture mechanics based interpretation of the load sequence effect in the flexural fatigue behavior of concrete using digital image correlation[J].Construction and Building Materials,2021,307.
19. F. S T ,Mariam G ,Abd M E , et al.Identification of Fracture Parameters of Fiber Reinforced Concrete Beams Made of Various Binders[J].Case Studies in Construction Materials,2021,(prepublish):e00573-.
20. Arash K ,Jorge B D .Influence of polypropylene fibres and silica fume on the mechanical and fracture properties of ultra-high-performance geopolymer concrete[J].Construction and Building Materials,2021,283.
21. Sanz B ,Planas J ,Sancho M J .Influence of corrosion rate on the mechanical interaction of reinforcing steel, oxide and concrete[J].Materials and Structures,2017,50(4).
22. Dong W ,Zhou X ,Wu Z , et al.Investigating crack initiation and propagation of concrete in restrained shrinkage circular/elliptical ring test[J].Materials and Structures,2017,50(1).
23. Tung D N ,Tue V N .A fracture mechanics-based approach to modeling the confinement effect in reinforced concrete columns[J].Construction and Building Materials,2016,102893-903.